

International Journal of Modern Physics: Conference Series
 © The Author(s)

Study of Open Systems with Molecules in Isotropic Liquids

Yasushi Kondo

*Department of Physics & Science and Technology Research Institute, Kindai University,
 Higashi-Osaka, Osaka 577-8502, Japan
 ykondo@kindai.ac.jp*

Masayuki Matsuzaki

*Department of Physics, Fukuoka University of Education,
 Munakata, Fukuoka 811-4192, Japan
 matsuz@fukuoka-edu.ac.jp*

Published Day Month Year

We are interested in dynamics of a system in an environment, or an open system. Such phenomena like *crossover* from Markovian to non-Markovian relaxation and *thermal equilibration* are of our interest. Open systems have experimentally been studied with ultra cold atoms, ions in traps, optics, and cold electric circuits because well isolated systems can be prepared here and thus the effects of environments can be controlled. We point out that some molecules solved in isotropic liquid are well isolated and thus they can also be employed for studying open systems in Nuclear Magnetic Resonance (NMR) experiments. First, we provide a short review on related phenomena of open systems that helps readers to understand our motivation. We, then, present two experiments as examples of our approach with molecules in isotropic liquids. Crossover from Markovian to non-Markovian relaxation was realized in one NMR experiment, while relaxation like phenomena were observed in approximately isolated systems in the other.

1. Introduction

A glass of cold beer becomes warm on a hot summer day. It is because the glass of beer interacts with its environment (often called a bath or lattice in some fields) and it is not an isolated system. It is an open system in the sense that it interacts with its environment. All the systems, except for the Universe itself, are not in principle isolated. Therefore, it is very important to understand an open system.

An open system has been studied as a problem of thermodynamics and statistical mechanics from Maxwell's age. However, most of studies were and are theoretical and experimental ones have only recently emerged. For example, a realization of *Maxwell's demon* was first reported as late as in 2010¹. This may be caused by the difficulty of controlling an environment: unknown factors are often attributed to

This is an Open Access article published by World Scientific Publishing Company. It is distributed under the terms of the Creative Commons Attribution 4.0 (CC-BY) License. Further distribution of this work is permitted, provided the original work is properly cited.

the environment. In order to obtain a well controlled environment, it is necessary to have a well isolated system and then to increase the interaction between the system and its environment in a controlled manner. Therefore, we now expect the advance of this field by experiments with ultra cold atoms², ions in traps³, optics⁴, and cold electric circuits⁵ because well isolated systems can be prepared with these systems. We, here, point out that some molecules solved in isotropic liquid are well isolated and thus they can also be employed for studying open systems.

Our idea to employ molecules solved in isotropic liquid for studying an open system comes from liquid-state Nuclear Magnetic Resonance (NMR) quantum computer experiments^{6,7}. NMR quantum computing (NMR-QC) is one of the several proposals for realizing a quantum computer. The spins of nuclei in molecules solved in isotropic liquid are employed as qubits. NMR-QC is based on the fact that these spins have long coherence times and thus a lot of quantum controls can be applied to them before losing their coherence. In other words, these are well isolated from their environment in the time scale of NMR experiments. This isolation can be measured with the spin-lattice relaxation times (T_1 's)⁸. They are characteristic times that the spins (= system) become thermal equilibrium because of interactions with their lattice (= environment) and are often larger than 10 s while the times required for basic quantum operations, such as CNOT⁹, are of the order of 1 ms. The inverses of the basic operation times are the scales of interaction strengths between these spins.

NMR-QC differs from other implementations of quantum computers in that it uses an ensemble of systems, or more than 10^{15} molecules^{6,7}, rather than a single system. This ensemble nature of NMR-QC makes difficult to implement a projection measurement although it is not impossible¹⁰. Therefore, the implementation of NMR-QC often requires some modifications from conventional quantum computing. Moreover, there are difficulties of scalability and pure-state preparation in NMR-QC⁹. We believe, however, that these difficulties in NMR-QC are not very essential when we employ molecules in isotropic liquid for studying an open system. First, an ensemble average is necessary for obtaining statistical knowledge and thus the ensemble nature of NMR can be a merit, rather than a demerit. Second, we are interested in studying experimentally a few-body system that is difficult to treat theoretically. Third, we employ molecules in isotropic liquid as a simulator of open systems and thus pseudo pure states⁹ are sufficient for our purpose.

2. Theoretical Background

In this section, we briefly review theoretical concepts and some experiments about phenomena called relaxation from an intuitive view point. In order to understand relaxation, the concept of an open system is important and an open system may be experimentally realized with two different approaches. The first is adding a well controlled environment on an isolated system. The second is making a system of interest and its environment in an isolated system. In any way, we paradoxically need

well, although approximately, isolated systems for these experiments. Therefore, we need to know some basic concepts of both open and isolated systems.

At the end of this section, we discuss our experimental target, an ensemble of molecules solved in isotropic liquid, as an ensemble of isolated systems.

2.1. Open System

A system of interest is interacting with its environment to a greater or less extent. Such a system is called to be *open* because there are information flows between the system and its environment. On the other hand, a system that is isolated from the rest is called a *closed* one.

2.1.1. Hamiltonian Description

The *degree of openness* depends on the interaction strength between the system of interest (S) and its environment (E) and on the time scale during which S is influenced by E . The dynamics of the total system (S and E) is determined by the total Hamiltonian

$$\mathcal{H} = \mathcal{H}_S + \mathcal{H}_I + \mathcal{H}_E, \quad (1)$$

where $\mathcal{H}_S, \mathcal{H}_I, \mathcal{H}_E$ are the Hamiltonian of S without the interactions with E , that of the interaction between S and E , and that of E without the interactions with S , respectively. The density matrix of the total system, ρ , is governed by the Liouville equation,

$$\frac{d\rho}{dt} = -i[\mathcal{H}, \rho], \quad (2)$$

where we take the natural unit system so that $\hbar = 1$. Its formal solution is

$$\rho(t) = U(t)\rho(0)U^\dagger(t), \quad (3)$$

where $U(t) = e^{-i\mathcal{H}t}$ and the time parameter t varies from 0 to T . T may be finite or infinite. We assume that \mathcal{H} is time independent. And then, the density matrix of S at t , $\rho_S(t)$, is given as

$$\rho_S(t) = Tr_E(\rho(t)), \quad (4)$$

where Tr_E denotes the operation of tracing out the environment freedom.

$\rho_S(t)$ is also described by the map Φ_t .

$$\rho_S(0) \rightarrow \rho_S(t) \stackrel{\text{def}}{=} \Phi_t \rho_S(0). \quad (5)$$

Φ_t must be *completely positive* and *trace preserving* since Φ_t describes the time development of ρ_S . Note that $\Phi_0 = I$ where I is the identity map. Therefore, Φ_t is described by the operator sum representation, as follows.

$$\Phi_t \rho_S(0) = \sum_i \Omega_i(t) \rho(0) \Omega_i^\dagger(t), \quad (6)$$

where Ω_i is an operator and $\sum_i \Omega_i(t) \Omega_i^\dagger(t) = I_S$, where I_S is the identity matrix in the system Hilbert space¹¹.

In experiments, targets under study are intended to be as isolated, or as decoupled, from their environments as possible so that they can be investigated without disturbances from environments. There are, however, always undesired interactions between them: these interactions make experiments complicated. Therefore, it is important to understand the open system characteristics. Moreover, if quantum mechanics is relevant in experiments, measurement devices are also considered to be a part of environment and thus understanding of the open system characteristics is very essential.

2.1.2. Information Flow in Open System

A system of interest (S) interacts with its environment (E) as discussed in § 2.1.1 and finally becomes, or *relaxes*, to a state in which the values of macroscopic quantities are stationary, universal with respect to different initial conditions, and predictable using statistical mechanics when the environmental degree of freedom is infinite. The final state must be a most probable (*typical* in the word of statistical mechanics) one. Independence of the final state on the initial one implies that S loses the information of its initial state. This *forgetting* mechanism is realized by transferring this information from S to E , or entangling S and E , by the interaction between them and then tracing out the freedom of E as shown in Eq. (4). This can be interpreted as the information loss of S by measuring with E ¹².

The final state that has perfectly lost the information of its initial state is, by definition of entropy, a maximal entropy state. The information flow from S to E leads S generically to thermalize towards the canonical mixed state¹³. This is called the General Canonical Principle. See also the references^{14,15}. It was stressed that an ensemble-averaging operation is not essential.

Let us consider a process towards a final state of S . Two qualitatively different processes exist¹¹.

2.1.3. Markovian Relaxation

Once the information of S flows into E , it never flows back to S . It is called a Markovian relaxation process.

We assume that there is no correlation between S and E at $t = 0$. A Markovian relaxation process can be approximately realized when the degree of freedom of the environment is large enough and when τ_S (the characteristic time of S) is much longer than τ_E (that of the environment).

In the case of Markovian relaxation process, the map Φ_t defined by Eq. (6) satisfies

$$\Phi_t(\Phi_{t'} \rho_S(t'')) = \Phi_{t+t'} \rho_S(t'')$$

or in short $\Phi_t \Phi_{t'} = \Phi_{t+t'}$ for $t, t' \geq 0$. Therefore,

$$\Phi = \{\Phi_t | 0 \leq t \leq T, \Phi_0 = I\}$$

forms a semigroup¹⁶. The above equation is interpreted as

$$\Phi_{t+\Delta t} \rho_S(0) = \rho_S(t + \Delta t) = \Phi_{\Delta t} (\Phi_t \rho_S(0)) = \Phi_{\Delta t} \rho_S(t). \quad (7)$$

Or, $\rho_S(t + \Delta t)$ is determined only by $\rho_S(t)$: the process is Markovian.

The master equation determines the time evolution of ρ_S is in the Lindblad form¹⁷.

$$\frac{d\rho_S}{dt} = \mathcal{L}\rho_S, \quad (8)$$

$$\mathcal{L} = -i[\mathcal{H}_S, \rho_S] + \sum_i \gamma_i \left(A_i \rho_S(t) A_i^\dagger - \frac{1}{2} \{A_i^\dagger A_i, \rho_S\} \right), \quad (9)$$

where A_i is a time independent operator and γ_i is a non-negative constant. A relaxation is caused by the dissipation, like friction, and stochastic terms¹².

2.1.4. non-Markovian Relaxation

The information of S flows into E and sometimes flows back to S . It is called a non-Markovian relaxation process.

This process is realized when there is correlation between S and E at $t = 0$, or when $\tau_S \gg \tau_E$ is not satisfied. It can also happen when the degree of freedom of E is not large enough. Since we assume that the system of interest has the finite degree of freedom and thus the total system has the finite degree of freedom, a recurrence in the total system dynamics is expected in a long term measurement according to the linearity of quantum mechanics.

A non-Markovian relaxation process implies that Φ is not a semigroup. In this case, the master equation determines the time evolution of ρ_S is very similar to the Lindblad form but different.

$$\frac{d\rho_S}{dt} = \mathcal{K}\rho_S, \quad (10)$$

$$\mathcal{K} = -i[\mathcal{H}_S(t), \rho_S] + \sum_i \gamma_i(t) \left(A_i(t) \rho_S(t) A_i(t)^\dagger - \frac{1}{2} \{A_i^\dagger(t) A_i(t), \rho_S\} \right), \quad (11)$$

where $\mathcal{H}_S(t)$ and $A_i(t)$ are time-dependent operators and $\gamma_i(t)$ may become negative. Note that we assume that the inverse of Φ_t , or Φ_t^{-1} , exists although Φ_t^{-1} is not necessarily positive.

2.1.5. Divisibility and Measure of non-Markovianity

Let us assume that Φ_t has an inverse Φ_t^{-1} for $t \geq 0$. We define a two parameter map

$$\Phi_{t,s} \stackrel{\text{def}}{=} \Phi_t \Phi_s^{-1}, \quad t \geq s \geq 0, \quad (12)$$

6 *Y. Kondo & M. Matsuzaki*

and $\Phi_{t,0}$ is defined by Φ_t . Then, $\Phi_{t,0}$ and $\Phi_{s,0}$ can be related as

$$\Phi_{t,0} = \Phi_{t,s}\Phi_{s,0}.$$

Φ_t is defined to be *P divisible* when $\Phi_{t,s}$ is positive. Similarly, it is *CP divisible* when $\Phi_{t,s}$ is completely positive. If Φ_t is *P divisible*, $\Phi_{t,s}$ corresponds to $\Phi_{\Delta t}$ in Eq. (7). And thus, *P divisible* Φ_t is Markovian. It is known that the reverse is true, too.

We now define non-Markovianity of the map Φ_t . Let us prepare an initial state ρ_S^1 with a probability p and another one ρ_S^2 with a probability $1 - p$. The operator Δ is defined as

$$\Delta \stackrel{def}{=} p\rho_S^1 - (1-p)\rho_S^2. \quad (13)$$

$\|\Delta\|$, where $\|\cdot\| = Tr\sqrt{*\dagger*}$, is considered as the distinguishability of the two states. If $\|\Phi_t\Delta\|$ monotonically decreases with t for all p and ρ_S^i combinations, Φ_t is said to be Markovian. Then, the measure of non-Markovianity is defined as

$$\mathcal{N}(\Phi) \stackrel{def}{=} \max_{p, \rho_S^i} \int_{\sigma > 0} \sigma dt, \quad (14)$$

where $\sigma(t) \stackrel{def}{=} \frac{d}{dt}\|\Phi_t\Delta\|$. If Φ_t is Markovian, $\sigma(t)$ is never positive and thus $\mathcal{N}(\Phi) = 0$. On the other hand, an information back flow causes an increase of $\|\Phi_t\Delta\|$ and thus $\sigma(t)$ becomes positive in some time interval: $\mathcal{N}(\Phi)$ becomes positive.

2.1.6. Collision Model

The collision model¹⁸ has been extended in order to model an open system that shows crossover from Markovian to non-Markovian relaxation according to its parameters¹⁹. We, here, discuss this extended model because it is very simple yet powerful and because it was successfully applied to an atom in a dissipative cavity for a Lorentzian spectral density of bath modes¹⁹. Our experiments with molecules in isotropic liquids^{10,20} may also be considered as realizations of variance of this extended collision model.

The environment in the original collision model¹⁸ is modeled as a large collection of non-interacting identical objects called ancillas. The system of interest, S , periodically interacts, or *collides*, with one of these ancillas. It is important that the collided ancilla will never collide S again: this guarantees the one-way information flow from S to the environment. By controlling the strength and frequency of these collisions, the relaxation rate of S can be controlled.

The ancilla interacts with S will disappear like in the original collision model but is allowed to *collide* another ancilla once, but only once, before disappearing in the extended collision model¹⁸. This another ancilla is the one that will interact with S next: this collision between ancillas provides the mechanism of memory in the environment. By controlling the collision between ancillas, the effect of memory can be controlled.

2.1.7. Photon Passing through a Quartz Plate

A photon is a well isolated system. It is “too” well-isolated that realization of a quantum computer with a photon is difficult⁹. We, here, review a photon passing through a quartz plate⁴: the polarization degree of freedom of photons $|\lambda\rangle$ ($\lambda = H, V$ and $H = \text{Horizontal}$ and $V = \text{Vertical}$) was a system of interest, S , while its frequency degree of freedom $|\omega\rangle$ as its environment. The spectrum of the photons, the initial state of the environment, was controlled by passing them through a Fabry-Pérot cavity. Their spectrum after the cavity depended on the incident angle to the cavity. Then, the interaction $U(t)$ between S and the environment was introduced by passing through a quartz plate as follows.

$$U(t) |\lambda\rangle \otimes |\omega\rangle = e^{in_\lambda \omega t} |\lambda\rangle \otimes |\omega\rangle,$$

where n_λ is the polarization depend refraction index of the photons. The interaction strength was controlled by changing the interaction time t , or the thickness of the quartz plate where the photons passed. Then, full state tomography of the photons was carried out with a single photon detector. Finally, the trace distance and concurrence between the “initial” and final state were analyzed and these quantities were found to show non-monotonic decrease, or non-Markovian behavior¹¹. Note that the “initial” state was not a real initial state because the single photon detector can only provide a destructive measurement. One of an entangled photon pair was measured to obtain the “initial” state while the other photon of the pair was employed for the above experiment and its final state was measured.

2.2. Isolated system

Dynamical chaos makes a system thermalize in classical statistical mechanics. An isolated quantum system, however, evolves linearly in time and the spectrum is discrete, and thus dynamical chaos itself cannot occur. It has been a long question how an isolated quantum system relaxes to a thermal state. Some important concepts are reviewed here²¹.

2.2.1. Eigenstate Thermalization Hypothesis

First of all, let us clarify the problem in relaxation of a quantum many-body system²². An integrable quantum system of which dynamics is determined by a few constants called integrals cannot, by definition, become thermalized because the initial state “memory” is kept in its dynamics. It is, however, that the condition of non-integrability is not sufficient.

Let us consider a dynamics of a quantum many-body system of which initial state $|\psi(0)\rangle$ and its energy is E_0 . It is expanded by the eigenvectors $|\Psi_\alpha\rangle$ of the system Hamiltonian \mathcal{H} as,

$$|\psi(0)\rangle = \sum_{\alpha} C_{\alpha} |\Psi_{\alpha}\rangle,$$

8 *Y. Kondo & M. Matsuzaki*

where $C_\alpha = \langle \Psi_\alpha | \psi(0) \rangle$ and we assume that \mathcal{H} is time independent and not degenerate for simplicity. The time evolution of $|\psi(t)\rangle$ is given as

$$|\psi(t)\rangle = \sum_{\alpha} C_{\alpha} e^{-i\mathcal{H}t} |\Psi_{\alpha}\rangle = \sum_{\alpha} C_{\alpha} e^{-iE_{\alpha}t} |\Psi_{\alpha}\rangle,$$

where E_{α} is an eigenvalue of $|\Psi_{\alpha}\rangle$. The expectation value of a few-body observable O is given as,

$$\langle O \rangle = \langle \Psi_{\alpha}(t) | O | \Psi_{\beta}(t) \rangle = \sum_{\alpha, \beta} C_{\alpha}^* C_{\beta} e^{i(E_{\alpha} - E_{\beta})t} O_{\alpha, \beta},$$

where $O_{\alpha, \beta} = \langle \Psi_{\alpha} | O | \Psi_{\beta} \rangle$. The long time average \bar{O} must relax to $\sum_{\alpha} |C_{\alpha}|^2 O_{\alpha, \alpha}$. It means that this must also be the ensemble average of O over the states of which energy is close to E_0 , or a microcanonical average of O .

$$\sum_{\alpha} |C_{\alpha}|^2 O_{\alpha, \alpha} \approx \bar{O} \approx \langle O \rangle_{\text{microcan}}(E_0) \stackrel{\text{def}}{=} \frac{1}{N_{E_0, \Delta E}} \sum_{|E_{\alpha} - E_0| < \Delta E} O_{\alpha, \alpha}, \quad (15)$$

where $N_{E_0, \Delta E}$ is the number of eigenstates within the energy window $[E_0 - \Delta E, E_0 + \Delta E]$. The selection of ΔE is not important as long as a lot of states exist in this window.

The problem is, now, clear: the left hand side of Eq. (15) depends on the initial state through C_{α} while there is no such dependence in the right hand side. In order to resolve this problem, it was conjectured that $O_{\alpha, \alpha}$ is approximately constant for the eigenstate $|\Psi_{\alpha}\rangle$ of which eigenvalue satisfies $|E_{\alpha} - E_0| < \Delta E$ ^{23,24}. This is called *eigenstate thermalization hypothesis* (ETH). ETH is summarized as follows.

The initial state of energy E_0 is a linear combination of the (energy) eigenstates of which eigenvalues are near E_0 . These eigenstates have the property of a thermal state but this property is not seen at first because of the coherence between them. However, this coherence disappears in time and the thermal state property appears. This is the thermalization of a quantum many-body system.

Although ETH is still a hypothesis, it seems to be quite reasonable and promising²².

2.2.2. Generalized Gibbs Ensemble

The term *equilibration* means that a system of interest undergoes relaxation to a state and stays there for a long time. An equilibrated state may depend on its initial state: this is different from thermalization. A certain system may become, or equilibrate to, a quasistationary state before thermalized. This phenomenon is called *prethermalization*^{25,26}. Such a quasistationary state is thought to be described as an generalized Gibbs ensemble (GGE) state that is a maximum entropy state with some constraints that related with the initial state, or conserved quantities = *integrals*.

It is worth noting that the term *integrable* is taken differently by researchers. In the reference²², it was stated that a quantum *integrable* system had conserved quantities of which number was much more than one but less than the dimension of its Hilbert space. On the other hand, this term was employed more restrictively like in the case of classical mechanics: a quantum *integrable* system had the same number of conserved quantities as that of the degrees of the freedom¹⁴. Depending on the usage, GGE systems are said to be either integrable or non-integrable.

Regardless of the usage of the term *integrable*, the GGE system does not thermalize because its integrals, or the information of the initial state, exist at $t \gg 1$.

2.2.3. Many-Body Localization

Many-body localization also prevents a system from thermalization²⁷. It is analogous to the well known Anderson localization²⁸ that a disordered potential make a single-particle wave function localize in real space. In contrast, the many-body localization occurs as a quasi particle localization in Fock space because of a random potential and interactions among components of the many-body system. A quasi particle localization means that the information of the initial state is also kept.

2.2.4. Scrambling

A concept recently attracting attention in connection with thermalization in quantum information and gravity fields is *scrambling*. Let us consider a quantum dynamics where initial states that are very similar but orthogonal with each other evolve to be quite different. Such a chaotic behavior is referred to as *scrambling*²⁹ and often called the quantum butterfly effect by comparing with its classical counterpart. The scrambling was originally discussed with a black hole: what happens for the information possessed by a falling object into a black hole when it crosses the event horizon? The information of the falling object is accessible before crossing but it is not after. Therefore, it is conjectured that a black hole is Nature's fastest scrambler³⁰.

2.2.5. Lieb-Robinson Bound

The Lieb-Robinson bound³¹ implies that the speed of information propagation in a non-equilibrium system has a certain limit. Such a propagation is also called the *light cone*-like information flow because it is similar to the propagation of light²¹ in the theory of relativity. It is formally described as follows. Let us consider two observables, O_1 and O_2 .

$$\|[O_1(t), O_2]\| \leq c \|O_1\| \|O_2\| \min\{|O_1|, |O_2|\} e^{-\mu(d(O_1, O_2) - v|t|)}, \quad (16)$$

where $\|\cdot\|$ is the operator norm, $d(O_1, O_2)$ the distance between the support of the observables, $|O_1|$ and $|O_2|$ the size of their supports, $v \geq 0$ is the velocity, and c and μ are positive constants.

The constant velocity propagation of the two-point parity correlation (information) was reported in the experiment with a one-dimensional quantum gas in an optical lattice³².

2.2.6. Out of Time Order Correlation (OTOC)

A special type of correlation functions, called out-of-time-order correlation (OTOC) function $F(\tau)$, has recently been attracting attention in order to quantify information, or entropy, flow and to probe scrambling of information³³. It is thus related to the Lieb-Robinson bound³⁴, too. Let us consider two unitary operators W and V that are commuting at time $\tau = 0$. Starting from $[W_\tau, V] = 0$ at $\tau = 0$, let us consider the change of $[W_\tau, V]$ in time τ and assume that it becomes non-zero. Here, $W_\tau = U_\tau^\dagger W U_\tau$ and $U_\tau = e^{-i\mathcal{H}\tau}$. It implies that W that is initially commuting with V becomes non-commuting after τ because of the interactions generated by \mathcal{H} .

The average of the square of $[W_\tau, V]$ is given as,

$$\langle |[W_\tau, V]|^2 \rangle = 2(1 - \Re[F(\tau)]) \quad (17)$$

$$\text{where } F(\tau) \stackrel{\text{def}}{=} \langle W_\tau^\dagger V^\dagger W_\tau V \rangle. \quad (18)$$

$F(\tau)$ is the out-of-time-order correlation function of W and V . In order to clarify the physical meaning of $F(\tau)$ and thus $\langle |[W_\tau, V]|^2 \rangle$, $F(\tau)$ is re-written as

$$F(\tau) = \langle O_B^\dagger(V, W, \tau) O_F(V, W, \tau) \rangle,$$

$$\text{where } O_F(V, W, \tau) \stackrel{\text{def}}{=} W U_\tau V,$$

$$O_B(V, W, \tau) \stackrel{\text{def}}{=} U_\tau V U_\tau^\dagger W U_\tau.$$

When W and V are properly selected, $F(\tau)$ has been proved to be equivalent to the second Rényi entropy^{35,36}. The Lyapunov exponent λ_L can also be defined with $1 - F(\tau) \propto e^{\lambda_L \tau}$ when W and V are hermitian. The OTOC in many-body systems can be employed in order to distinguish a many-body localized phase from an Anderson localized one while a normal correlation function cannot³⁶.

Although the OTOC function, $F(\tau)$, is very useful, its measurement is not trivial for a many-body quantum system because of the time reversal operation U_τ^\dagger appeared in $O_B(V, W, \tau)$. Despite of the difficulty, some OTOC's, however, have been measured in a NMR³⁷ and trapped ion³⁸ experiments.

2.2.7. The Second Law of Thermodynamics in Closed System

Equilibrium thermodynamics is based on the fact that the system of interest is contact with the canonical bath, or environment. The second law means that the system evolves quasistatically in such a way that its entropy increases. The increase of entropy indicates the information flow from the system to the environment.

The second law of thermodynamics, and also the fluctuation theorem, in a closed and pure system have been discussed³⁹. This closed system consists of the system

of interest, S , and its environment. It was pointed out that the second law of thermodynamics is applicable for S with some error even if the environment, that is a part of the closed system, is not a canonical bath, but if it is an energy eigenstate and the weak ETH is satisfied. Here, “weak” means “less restrictive”³⁹. This conclusion is based on the fact that S cannot distinguish a weak ETH environment from the canonical bath because the speed of the information flow (the Lieb-Robinson bound³¹) is limited and thus enough information for distinguishing them cannot be collected within a limited time.

2.3. molecules solved in isotropic liquid as isolated systems

Molecules solved in liquid are under influence of solvent molecules. In principle, the nuclear spins in the molecule consist of an open system, as shown in Fig. 1 (a). We, however, have to take into account that molecules in isotropic liquid

- are under an external strong magnetic field, and
- are rapidly moving.

The strong external magnetic field dominates the spin dynamics and thus simplifies it. Or, the original Hamiltonian which determines the spin dynamics may be replaced by a more simpler one: secular approximation⁸. On the other hand, the rapid molecular motion causes interactions to fluctuate in time. The fluctuating interaction may be replaced by its time averaged one: motional averaging⁸.

The secular approximation and motional averaging make effective interactions much simpler than the original ones in molecules solved in isotropic liquids⁸.

- Intramolecular interactions are described as

$$\mathcal{H} = \sum_j \omega_{0,j} \frac{\sigma_{z,j}}{2} + \sum_{j < k} J_{j,k} \frac{\vec{\sigma}_j \cdot \vec{\sigma}_k}{4} \quad (19)$$

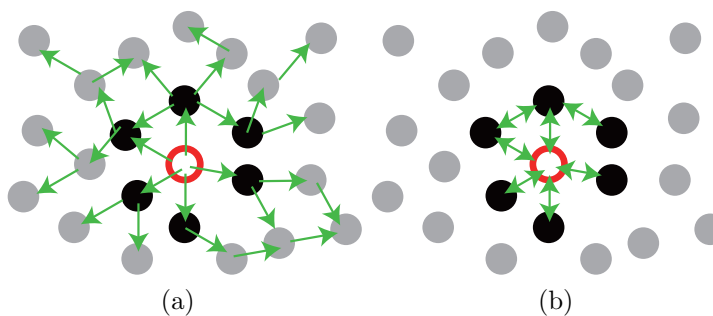


Fig. 1. Molecules in liquids. The arrows indicate the flow of information originally in the red open circle spin, or interactions among nuclear spins, in the molecules and liquids. The red and black spins consist of the molecule, while the gray ones are spins in liquids. (a) Open system, or the information flows into the liquid. (b) Closed system, or the information stays inside of the molecule.

where

$$\vec{\sigma}_i = \overbrace{I \otimes I \otimes \cdots \otimes I}^{1 \sim i-1} \otimes \vec{\sigma} \otimes \overbrace{I \otimes I \otimes \cdots \otimes I}^{i+1 \sim n}, \quad \text{and} \quad \vec{\sigma} = (\sigma_x, \sigma_y, \sigma_z).$$

σ_k is a standard Pauli matrix, $\omega_{0,j}$ the isotropic chemically shifted Larmor frequency of the j 'th spin, and $J_{j,k}$ the interaction strength between the j 'th and k 'th spins. $J_{j,k}$ is often measured in Hz in NMR textbooks, but it is measured in rad/s as $\omega_{0,j}$ here.

- Interactions among spins inside and outside molecules are dipole-dipole interactions.

If the dipole-dipole interactions among spins inside and outside molecules could be ignored, the spins in the molecules are regarded as an isolated spin system⁸, as shown in Fig. 1 (b). We also note that the strength of the intermolecular dipole-dipole interaction can be evaluated by measuring T_1 because this flips the spin in the molecule and causes the spin-lattice relaxation.

Therefore, molecules in isotropic liquids investigated with NMR may be approximately isolated from the environment, their Hamiltonian is simple, and they are able to be measured with NMR techniques.

3. Experiments

We have been working on molecules in isotropic liquids with NMR: we have employed them in order to study ideas of quantum computation⁴⁰, robust quantum controls^{41,42}, Bang-Bang controls²⁰, and so on. Our NMR spectrometer is a standard one for precise chemical analysis, or JEOL ECA-500.

We, here, present experiments in which molecules in isotropic liquid are regarded as an ensemble of isolated, at least approximately, systems. An ensemble of cold atoms is regarded as a well isolated system^{2,21} and the isolated system has often been theoretically studied with the cold atoms in mind. In this section we point out that an ensemble of molecules in isotropic liquid, which is much easier to treat, is also a good model to study an isolated system. We note that molecules in isotropic liquid can simulate quantum registers in quantum computation and that their dynamics is approximately unitary, at least in a short time. In other words, some molecules in isotropic liquids are widely accepted as approximately isolated systems^{6,7}.

We recommend a reader who is not familiar with NMR to refer a standard NMR textbook, such as one by Levitt⁸. We also provided a crash course of NMR for NMR quantum computation^{43,44} which may be a convenient start point. The concept of our experiments is discussed in § 3.1. The state, or information, of a part of this molecule is characterized by its transverse magnetization and its dynamics after an abrupt change is tracked with NMR techniques. Then, our experiments are summarized in § 3.2 and 3.3.

3.1. Relaxation Experiments with Molecules in Isotropic Liquids

We designed two types of experiments: *realization of the extended collision model* and *a system and environment in an isolated molecule*.

3.1.1. Density Matrix and Free Induction Decay Signal

We performed two kinds of relaxation experiments. The information that we tracked in our experiments was the transverse magnetization of one of the nuclear spins in the molecule, perpendicular to the applied strong static magnetic field. From the quantum mechanical view, the thermally equilibrium density matrix ρ_{th} of a molecule in isotropic liquid at room temperature T , see the Hamiltonian (19), is well approximated as

$$\rho_{\text{th}} = \left(\frac{I}{2}\right)^{\otimes n} + \sum_j \frac{\omega_{0,j}}{2k_B T} \frac{\sigma_{z,j}}{2^n} \quad (20)$$

because the thermal energy $k_B T$ is much larger than that of magnetic ones $\omega_{0,j}$ and because the energies associated with the interactions $J_{i,j}$ are even much smaller than the magnetic ones^{8,43,44}. Let us assume that we measure the first spin and then ρ_{th} can be rewritten as

$$\rho_{\text{th}} = \left(\frac{I}{2}\right)^{\otimes n} \left(1 - \frac{\omega_{0,1}}{2k_B T}\right) + \frac{\omega_{0,1}}{2k_B T} \begin{pmatrix} 1 & 0 \\ 0 & 0 \end{pmatrix} \otimes \frac{I^{\otimes(n-1)}}{2^{n-1}} + \sum_{j \neq 1} \frac{\omega_{0,j}}{2k_B T} \frac{\sigma_{z,j}}{2^n}.$$

Note that $(I/2)^{\otimes n}$ is not visible in NMR because $\text{Tr}(\vec{\sigma}_j(I/2)^{\otimes n}) = \vec{0}$. Then, we apply the operation $R(\pi/2, \pi/2) \otimes I^{\otimes(n-1)}$ on ρ_{th} , where

$$R(\beta, \phi) \stackrel{\text{def}}{=} e^{-i\beta(\cos \phi \sigma_x + \sin \phi \sigma_y)/2}. \quad (21)$$

This rotates the first spin magnetization by the angle β around the axis in the xy -plane with an angle ϕ from the x -axis. This operation can be realized by applying a rotating, or equivalently oscillating, magnetic field of which frequency is $\omega_{0,1}$ for a certain period^{8,43,44}. We obtain the following initial state

$$\rho(0) = \frac{1}{2} \begin{pmatrix} 1 & 1 \\ 1 & 1 \end{pmatrix} \otimes \frac{I^{\otimes(n-1)}}{2^{n-1}} \quad (22)$$

by re-normalizing $\frac{\omega_{0,j}}{2k_B T} \rightarrow 1$. We neglect $(I/2)^{\otimes n}$ and the other spin terms since they are not observable.

Let us consider the dynamics in the frame where spins are seen in their own rotating frame of which frequencies are their Larmor ones. In this frame, Hamiltonian (19) is reduced to

$$\mathcal{H} = \sum_{j < k} J_{j,k} \frac{\sigma_{z,j} \sigma_{z,k}}{4}, \quad (23)$$

if we assume that $|\omega_{0,j} - \omega_{0,k}| \gg |J_{j,k}|$ for our molecules. This assumption is called the weak coupling limit⁸.

We observe the relaxation process, or more precisely dephasing one, of the spin 1 under the Hamiltonian (23). When the freedom of the other spins are traced out, the density matrix of the spin 1, $\rho_1(t)$, can be described as

$$\rho_1(t) = n_x(t) \frac{\sigma_x}{2} + n_y(t) \frac{\sigma_y}{2} + \frac{I}{2}.$$

Note that the diagonal terms are constant under Hamiltonian (23). A complex Free Induction Decay (FID) signal $S(t)$ is given as

$$S(t) = n_x(t) + i n_y(t) = \text{Tr}((\sigma_x + i \sigma_y) \rho_1(t)). \quad (24)$$

Thus, $n_x(t)$ and $n_y(t)$ are called the real and imaginary part of the complex FID signal, respectively. For example, $S(0) = 1$, while the perfectly dephased state $\rho_1(\infty) = \frac{1}{2}I$ gives $S(\infty) = 0$. The trace distance between $\rho_1(t)$ and $\rho_1(\infty)$, $D(\rho_1(t), \rho_1(\infty))$, is given as

$$\begin{aligned} D(\rho_1(t), \rho_1(\infty)) &\stackrel{\text{def}}{=} \frac{1}{2} \text{Tr} \left(\sqrt{(\rho_1(t) - \rho_1(\infty))^\dagger (\rho_1(t) - \rho_1(\infty))} \right) \\ &= \frac{1}{2} \sqrt{n_x^2(t) + n_y^2(t)}, \end{aligned} \quad (25)$$

and thus $S(t)$ is a good measure of the trace distance in our experiments where we observe the dephasing.

3.1.2. Decoupling

There is a very interesting technique in NMR called decoupling⁸. The interaction strengths inside molecules in isotropic liquids are usually of the order of 100 Hz or less in frequency unit. Therefore, if one can flip-flop the spins much faster than these frequencies, for example by applying rf pulses on them, these spins are nullified in average. We employed this technique in order to control the number of effective (active) spins in the molecule.

3.1.3. Realization of the Extended Collision Model

The extended collision model¹⁹ may be re-formulated as follows. The system of interest, S , frequently collides one ancilla. If this ancilla is reset before next collision with S , the information flow is one-way and thus S shows a Markovian relaxation. A large collection of ancillas is not necessary. If the reset of the ancilla is not perfect, or if the interval τ_{reset} between resetting the ancilla is large so that the information backflow occurs, the ancilla provides the mechanism of memory of the environment. S may show a non-Markovian relaxation.

Our reported experiments with chloroform molecules^{10,20} may be considered as a faithful realization of the above re-formulated extended collision model. The ^{13}C nuclear spin is S while the hydrogen one corresponds to the ancilla. Note that chlorine nuclear spins are magnetically inert. The resetting mechanism is provided

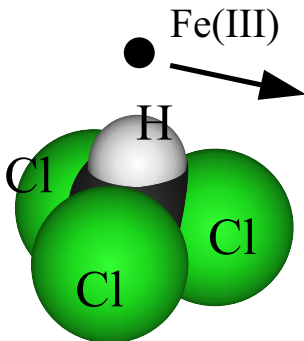


Fig. 2. Realization of the extended collision model with a chloroform molecule and Fe(III) magnetic impurity. The ^{13}C nuclear spin is S while the hydrogen one corresponds to the ancilla. Note that chlorine nuclear spins are magnetically inert. The resetting mechanism is provided by randomly moving Fe(III) paramagnetic impurities.

by randomly moving Fe(III) paramagnetic impurities. See Fig. 2. Because of r^{-3} dependence of the dipole field generated by the Fe(III) magnetic impurities, where r is the distance from it, the ^{13}C nuclear spin is approximately not influenced by the Fe(III) impurities compared with the hydrogen spin. τ_{reset} is of the order of its longitudinal relaxation time $T_{1,\text{H}}$. The Hamiltonian that determines the spin dynamics of the chloroform molecule is $\mathcal{H} = J \frac{\sigma_z \otimes \sigma_z}{4}$, where $J = 2\pi \cdot 215 \text{ rad/s}$, and thus the time scale of the spin dynamics is of the order of $\frac{2\pi}{J}$. See also Eq. (23).

Therefore, the frequentness of the resetting the ancilla is measured with $\frac{2\pi}{JT_{1,\text{H}}}$. More rigorous treatment with the operator sum representation^{9,45,46} can be found in our previous publications^{10,20}.

In this work, we show the experiments with tetramethylsilane (TMS) molecules with a small J in order to demonstrate non-Markovian to Markovian crossover of relaxation. The small J means that $\frac{2\pi}{JT_{1,\text{H}}}$ can be large with the same $T_{1,\text{H}}$.

3.1.4. System and Environment in an Isolated Molecule

We also design other experiments by employing molecules in isotropic liquids as an ensemble of isolated systems. An interacting nuclear spin system in one isolated molecule is divided into two parts. One of them is treated as a system of interest. We are inspired by the experiments with ultra cold atoms that form a well isolated system, but we are interested in the behavior of a finite system. We are interested in the minimum size of the left that is able to act as environment of the first.

We employed ^{13}C enriched transcrotonic-acid and normal 4,4-dimethyl-4-silapentane-1-sulfonic acid (DSS) molecules. DSS is very popular as a frequency standard in NMR experiments.

3.2. Realization of the Extended Collision Model

3.2.1. Less Frequent Resetting

We employed tetramethylsilane (TMS) of which molecular structure is shown in Fig. 3 (a). This molecule is often employed for the frequency standard of ^{13}C and hydrogen and is very popular in standard NMR experiments. The natural abundance of the silicon isotope ^{29}Si of which spin is $1/2$ and active in NMR is about 5 % and thus these spins are easily measured with NMR. We assigned the center silicon nuclear spin (^{29}Si) as the system of interest S , while the twelve hydrogen spins are ancillas. Our sample is not ^{13}C enriched and thus we can ignore the carbon spins because its natural abundance of ^{13}C is only 1 %. The interaction network is shown in Fig. 3 (b). It is very simple because the molecular structure is very symmetric. The interaction strength is $2\pi \cdot 6.6$ rad/s which is much smaller than that of chloroform. There are no interactions among hydrogen spins because of the symmetry.

The sample is a mixture of 2.89 g normal (neither ^{13}C nor ^{29}Si is enriched) tetramethylsilane and 2.53 g acetone- d_6 (deuterized acetone). T_1 of silicon spin is 16 s and that of hydrogen is 10 s. Therefore, this molecule is well isolated from the solvent in the time scale of few tenths of second.

The FID signal of the central silicon nuclear spin is shown in Fig. 4. The FID signal is a good measure of the trace distance $D(\rho_1(t), \rho_1(\infty))$ as discussed with Eqs. (24, 25). The FID signal shows revivals which indicate that the information originally at the silicon spin moves to the surrounding hydrogen spins and then flows back to the silicon spin again and again. More than ten revivals are seen.

This experimental result can be interpreted as follows: The hydrogen spins (= ancillas) are not frequently reset (large $T_{1,H}$) and thus the environment well *remembers* the history of the interaction with the system of interest.

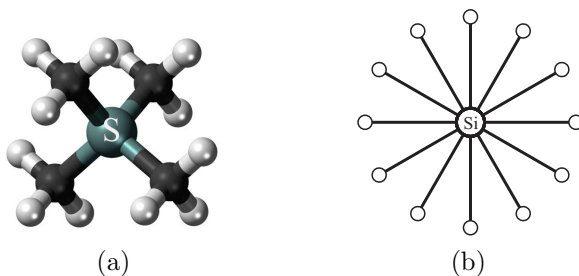


Fig. 3. Tetramethylsilane (TMS). (a) Structure. The center sphere marked S is a silicon, the four black ones are carbon, and the twelve white ones are hydrogen atoms, respectively. (b) Interaction network. The silicon spin equally interacts with the twelve hydrogen spins represented with small circles because of the molecular structure symmetry. The carbon spins can be ignored because they are not ^{13}C enriched.

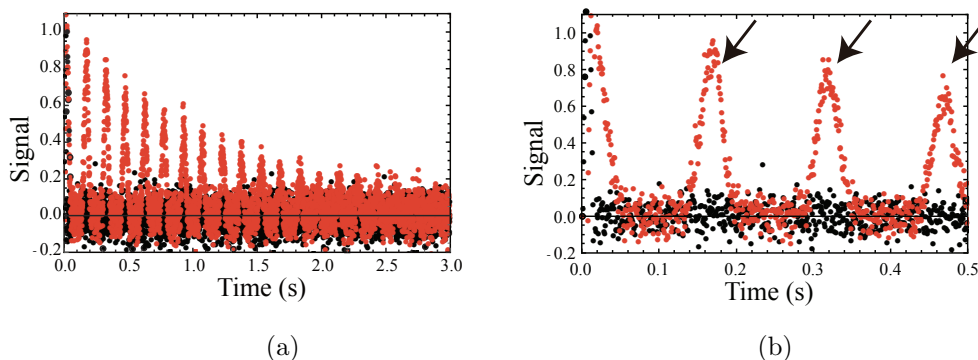


Fig. 4. FID signal of silicon spin in tetramethylsilane molecule. The red (black) points are the real (imaginary) part of the complex FID signal. (a) More than ten times revivals are seen. (b) The first 0.5 s of the FID signal is shown.

3.2.2. Frequent Resetting

We introduced the resetting mechanism by adding some magnetic impurities, as we discussed. We prepared two samples with magnetic impurities of 19 mM and 40 mM. Their T_1 's of silicon spins are 2.6 s (19 mM) and 1.4 s (40 mM). Therefore, the direct influence of the magnetic impurity can approximately be ignored in the first few tenths of a second. On the other hand, $T_{1,H}$'s are 140 ms (19 mM) and 70 ms (40 mM) and are much shorter than the time scale determined by the interaction strength $2\pi \cdot 6.6$ rad/s: it implies that resetting the ancillas is very frequent. We also conclude that the magnetic impurities independently reset ancillas because $(T_1 \times \text{impurity concentration})$ is constant²⁰.

Revivals are not visible with the 40 mM sample, while the small revival is seen with the 19 mM one, as shown in Fig. 5. It can be interpreted as follows: resetting ancillas is frequent enough so that the information flow becomes one-way, or the system of interest in the 40 mM sample shows a Markovian relaxation. We observe the crossover from non-Markovian to Markovian relaxation by increasing the concentration of the magnetic impurities.

3.3. System and Environment in an Isolated Molecule

3.3.1. Molecules with large degrees of freedom

We employed ^{13}C -enriched transcrotonic-acid and normal 4,4-dimethyl-4-silapentane-1-sulfonic acid (DSS) molecules solved in heavy water as an approximately isolated molecules with large degrees of freedom. Their molecular structures are shown in Fig. 6. The number of spins in ^{13}C -enriched transcrotonic-acid is nine, while that of normal DSS fifteen. Note that the natural abundance of ^{16}O without spin is almost 100 % and that the hydrogens in the carboxy and sulfo group in Fig. 6 are detached in water.

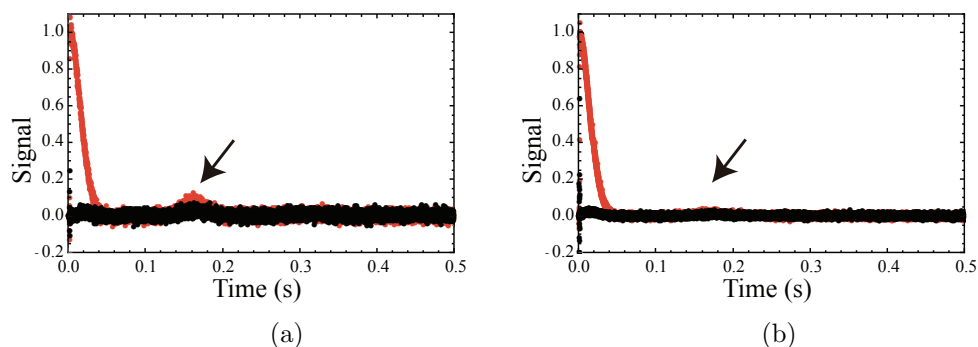


Fig. 5. FID signals with Fe(III) impurities of (a) 19 mM and (b) 40 mM. The crossover from non-Markovian to Markovian relaxation is observed in increasing the concentration of Fe(III), or the frequency of resetting. See, also Fig. 4 (b) for comparison.

The ^{13}C -enriched transcrotonic-acid molecule has often been employed in NMR quantum computer experiments⁴⁷. In other words, this molecule has been accepted to be a well isolated spin system. What is interesting with the DSS molecule is similarity in its molecular structure with that of TMS. TMS is usually employed in NMR experiments as a frequency standard in organic solvents, while DSS in water. When one of the hydrogen atoms in TMS is replaced with a carbon chain which has a sulfo group at the end, DSS is obtained. This carbon chain makes DSS solvable in water. On the other hand, this modification in molecular structure increases the degree of freedom in our experimental point of view since the molecular structure of DSS is less symmetric than that of TMS. It is noteworthy that the degree of freedom of the TMS molecule is not so large compared with ^{13}C -enriched transcrotonic-acid or normal DSS because of the symmetry of TMS molecule although the number of spins in it is as large as thirteen.

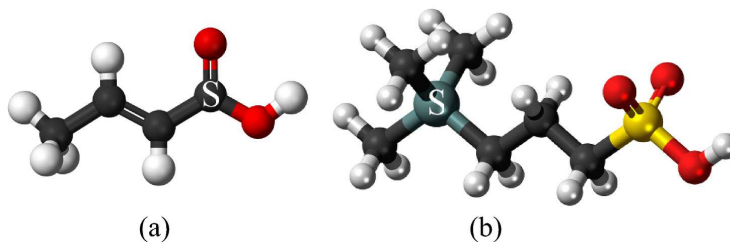


Fig. 6. Molecular structures of (a) transcrotonic-acid and (b) normal 4,4-dimethyl-4-silapentane-1-sulfonic acid. The spheres marked S are the systems of interest. S in the transcrotonic acid molecule is a ^{13}C spin in the carboxy group, while that in the DSS molecule a silicone spin. The black spheres are carbon, the white ones are hydrogen, the red ones are oxygen, and the yellow one is sulfa, respectively. The numbers of interacting spins are nine (fifteen) in the transcrotonic acid (DSS).

T_1 's of ^{13}C in the transcrotonic acid solved in D_2O (about 70 mM) were 8 s (methyl group), 10 s, 10 s, and 14 s (carboxy group) from left to right in Fig. 6 (a), while those of the hydrogen spins were 4 s (methyl group), 6 s, and 6 s. On the other hand, T_1 's of ^{29}Si in DSS (0.083 g solved in 0.74 g of D_2O) were 7 s, while those of the hydrogen spins were 3 s (methyl group) and 1.5 s (the others) in Fig. 6 (b). We concluded that both the transcrotonic acid and DSS molecules are well isolated in the first few tenths of a second of FID signals.

3.3.2. DSS

We performed experiments with the DSS molecule, shown in Fig. 6 (b), as that with the large degree of freedom. Figure 7 (a, b) show the interaction networks with and without hydrogen decoupling. There is a very large difference between them. Figure 7 (c) shows the FID signal of the silicon spin when all hydrogen spins were decoupled. In this case, the number of the spins in the molecule was effectively one, only the silicon spin. The signal decay indicates that the molecule was not perfectly isolated from the environment. One can, however, state that it was approximately isolated in a short time scale of 0.1 s.

The FID signal of the silicon spin is shown in Fig. 7 (d) when all hydrogen spins were active. This FID signal is very different from that with decoupling (Fig. 7 (c)) or that of TMS (Fig. 4). If we stopped the measurement of the FID signal at 0.1 s, we might conclude that the silicon spin relaxes perfectly. In other words, the finite system of the 15 hydrogen spins act as environment for the silicon spin and induces relaxation of the silicon spin within 0.1 s. On the other hand, we can clearly see a revival at 0.3 s although it is very small compared with those observed in the FID signal of TMS. We interpret that the information flows into the carbon chain, reflected at its end, and flows back to the silicon nuclear spin. In other words, we observe the finite speed of the information flow, or the Lieb-Robinson bound³¹. The interaction strengths between the hydrogen nuclear spins in the carbon chain, measured from the spectra of the hydrogen spins, are of the order of $2\pi \cdot 10$ rad/s and consistent with the revival at 0.3 s.

3.3.3. Transcrotonic Acid

We employed the transcrotonic acid molecule, shown in Fig. 6 (a), in order to demonstrate the influence of the degree of freedom on the information flow.

Figure 8 shows the ^{13}C spectrum obtained after operating $R(\pi/2, \pi/2)^{\otimes 4}$ on ρ_{th} by applying a short rf-pulse on all ^{13}C spins and when all hydrogen spins were decoupled. Close view of the peak marked S, see the inset of Fig. 8, reveals that it consists of two groups of peaks and each group consists of two peaks: four peaks in total. These four peaks correspond to four different states of No. 2 and 3 ^{13}C spins, or $|00\rangle$, $|01\rangle$, $|10\rangle$, and $|11\rangle$.

We employed another NMR technique called a soft pulse⁸. A Gaussian envelope

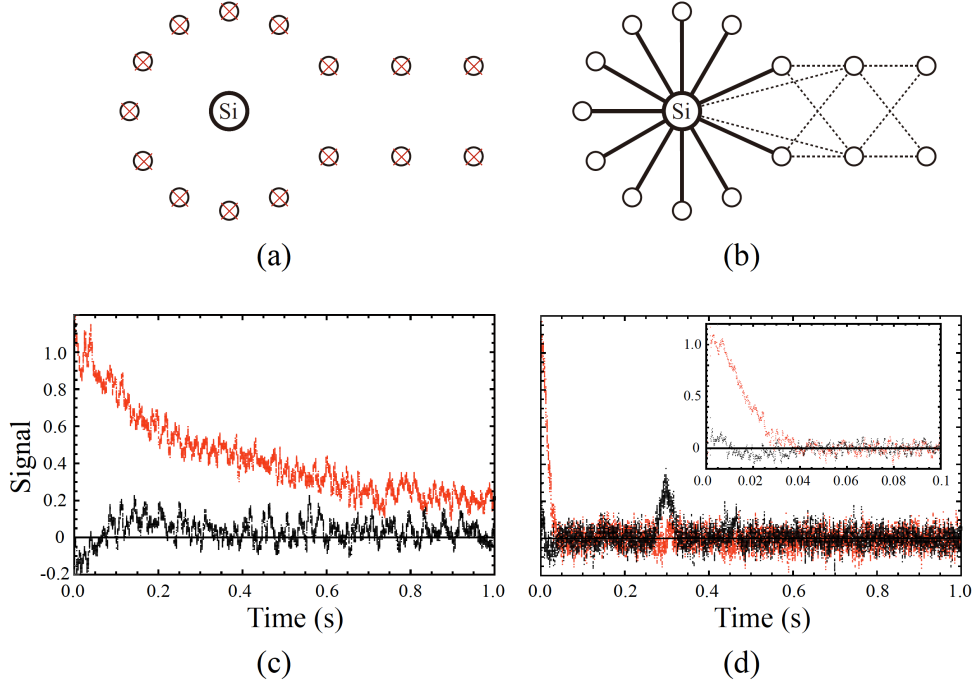


Fig. 7. Interaction networks (a, b) and FID signals (c, d) of DSS in D_2O . The FID signals of the silicon spin in DSS were measured. (a, c) All hydrogen spins are nullified. (b, d) All spins are active and thus the number of degrees of freedom is large. (d) The inset shows the first 0.1 s of the FID signal. The thick solid (thin dotted) lines in (b) represent interactions through one (two) carbon atom(s). The small circles represent hydrogen spins.

pulse with as long as 40 ms duration can turn the only magnetization at 169.4 ppm in Fig. 8. The state that we obtained was

$$\rho_{\text{ini}} = \frac{1}{2} \begin{pmatrix} 1 & 1 \\ 1 & 1 \end{pmatrix} \otimes \begin{pmatrix} 0 & 0 \\ 0 & 1 \end{pmatrix} \otimes \frac{I^{\otimes(n-2)}}{2^{n-2}},$$

where n is the total number of active spins. If the hydrogen spins were decoupled, $n = 4$. On the other hand, $n = 9$ if the hydrogen spins were active. The first spin is the ^{13}C in the carboxy group. Then, the information (transverse magnetization) flows into the spin chain.

Figure 9 (a, b) show the interaction networks. The interaction network with the hydrogen spins (b) is much more complicated than that without the hydrogen spins (a). It implies that the degree of freedom of (b) is much larger than that of (a). The FID signals of the ^{13}C nuclear spin in the carboxy group are shown in Fig. 9 (c, d) with and without hydrogen decoupling, respectively. Large revivals are seen in Fig. 9 (c), while they are much smaller in Fig. 9 (d). The more degrees of freedom, the smaller revivals.

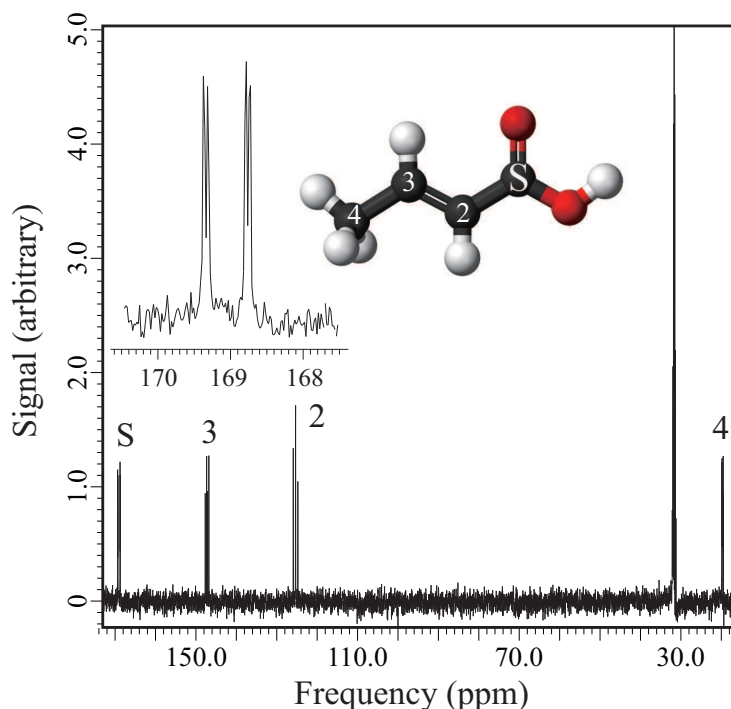


Fig. 8. Spectrum of transcrotonic acid in D_2O after a short rf-pulse that rotates all ^{13}C spins into the xy -plane when all hydrogen spins were decoupled. The peaks and the ^{13}C spins in the molecular model are corresponded by number. The peak at 33 ppm may be originated from some impurity. The detailed structure of the peak marked S is shown in the inset. See the text for more details.

4. Conclusions

We first very briefly discussed the basic ideas related with relaxation phenomena that should be a good start point for a person who is interested in them. We, however, recommend serious readers to refer, at least, the papers listed here and references therein. We also apologize to the readers for our not-comprehensive reference list. We then provided our experimental results with molecules in isotropic liquids as one unique experimental approach to investigating relaxation phenomena. We employed these molecules as isolated few body systems.

We believe that our approach may be interesting and effective because there are various molecules available and because experiments can be done with a standard commercial NMR equipment. Only the idea is important and no difficult experimental techniques are required. These experiments must complement those with ultra cold atoms², ions in traps³, optics⁴, and cold electric circuits⁵.

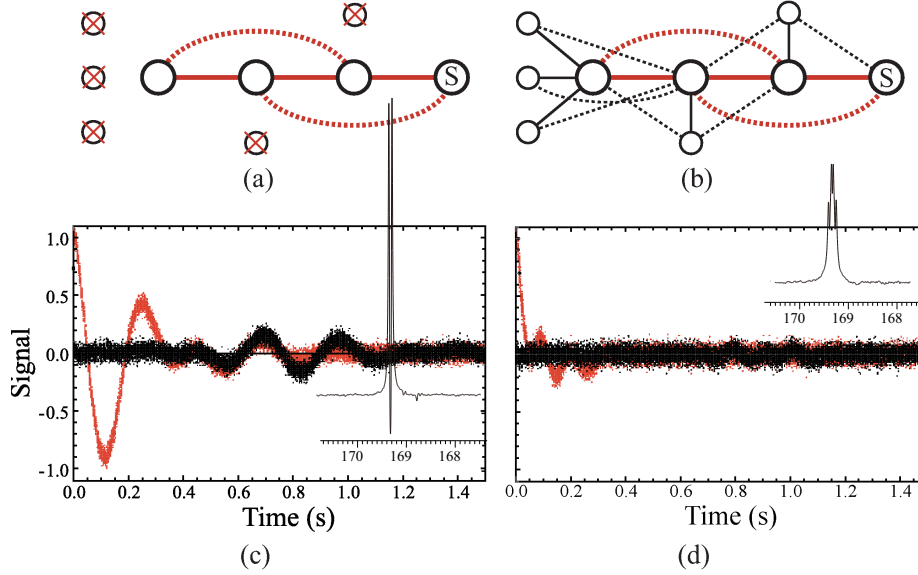


Fig. 9. Interaction networks (a, b) and FID signals (c, d) of transcrotonic acid in D_2O . The large circles represent ^{13}C nuclear spins, while the small ones hydrogen nuclear spins. The red thick (black thin) lines represent interactions between ^{13}C – ^{13}C (^{13}C –hydrogen). The solid (dotted) lines represent the nearest (next nearest) interactions. The FID signals of the ^{13}C nuclear spin (marked S) in the carboxy group were measured. (a, c) All the hydrogen nuclear spins are decoupled, or the degree of freedom is small. The large revivals are seen. (b, d) All the spins are active and thus the degree of freedom is large. The revivals are smaller. The spectra correspond to these FID signals are also shown in the insets. Note that there is no peak at 168.8 ppm.

acknowledgments

We would like to thank Hayato Nakano for participating in fruitful discussions. YK would like to thank a partial support of JST CREST Grant Number JPMJCR1774.

References

1. S. Toyabe, T. Sagawa, M. Ueda, E. Muneyuki and M. Sano, *Nature Physics* **6**, 988 EP (11 2010).
2. A. Polkovnikov, K. Sengupta, A. Silva and M. Vengalattore, *Rev. Mod. Phys.* **83**, 863 (Aug 2011).
3. D. Leibfried, R. Blatt, C. Monroe and D. Wineland, *Rev. Mod. Phys.* **75**, 281 (Mar 2003).
4. B.-H. Liu, L. Li, Y.-F. Huang, C.-F. Li, G.-C. Guo, E.-M. Laine, H.-P. Breuer and J. Piilo, *Nature Physics* **7**, 931 EP (09 2011).
5. J. P. Pekola, *Nature Physics* **11**, 118 EP (02 2015).
6. D. G. Cory, A. F. Fahmy and T. F. Havel, *Proceedings of the National Academy of Sciences* **94**, 1634 (1997).
7. N. A. Gershenfeld and I. L. Chuang, *Science* **275**, 350 (1997).
8. M. Levitt, *Spin Dynamics: Basics of Nuclear Magnetic Resonance* (Wiley, 2008).
9. M. Nielsen and I. Chuang, *Quantum Computation and Quantum Informa-*

- tion Cambridge Series on Information and the Natural Sciences, Cambridge Series on Information and the Natural Sciences (Cambridge University Press, 2000).
10. Y. Kondo, Y. Matsuzaki, K. Matsushima and J. G. Filgueiras, *New Journal of Physics* **18**, p. 013033 (2016).
 11. H.-P. Breuer, E.-M. Laine, J. Piilo and B. Vacchini, *Rev. Mod. Phys.* **88**, p. 021002 (Apr 2016).
 12. W. H. Zurek, Decoherence abd the transition from quantum to classical — revised, Los Alamos Science Number 27, (2002).
 13. S. Popescu, A. J. Short and A. Winter, *Nature Physics* **2**, 754 EP (Oct 2006), Article.
 14. C. Gogolin, M. P. Müller and J. Eisert, *Phys. Rev. Lett.* **106**, p. 040401 (Jan 2011).
 15. N. Linden, S. Popescu, A. J. Short and A. Winter, *Phys. Rev. E* **79**, p. 061103 (Jun 2009).
 16. K. L. Robert Alicki, *Quantum Dynamical Semigroups and Applications*, Lecture Notes in Physics, Vol. 717, 1 edn. (Springer-Verlag Berlin Heidelberg, 2007).
 17. Á. Rivas, S. F. Huelga and M. B. Plenio, *Reports on Progress in Physics* **77**, p. 094001 (2014).
 18. J. Rau, *Phys. Rev.* **129**, 1880 (Feb 1963).
 19. F. Ciccarello, G. M. Palma and V. Giovannetti, *Phys. Rev. A* **87**, p. 040103 (Apr 2013).
 20. A. Iwakura, Y. Matsuzaki and Y. Kondo, *Phys. Rev. A* **96**, p. 032303 (Sep 2017).
 21. J. Eisert, M. Friesdorf and C. Gogolin, *Nature Physics* **11**, 124 EP (02 2015).
 22. M. Rigol, V. Dunjko and M. Olshanii, *Nature* **452**, 854 EP (04 2008).
 23. J. M. Deutsch, *Phys. Rev. A* **43**, 2046 (Feb 1991).
 24. M. Srednicki, *Phys. Rev. E* **50**, 888 (Aug 1994).
 25. M. Kollar, F. A. Wolf and M. Eckstein, *Phys. Rev. B* **84**, p. 054304 (Aug 2011).
 26. M. Gring, M. Kuhnert, T. Langen, T. Kitagawa, B. Rauer, M. Schreitl, I. Mazets, D. A. Smith, E. Demler and J. Schmiedmayer, *Science* **337**, 1318 (2012).
 27. R. Nandkishore and D. A. Huse, *Annual Review of Condensed Matter Physics* **6**, 15 (2015).
 28. P. W. Anderson, *Phys. Rev.* **109**, 1492 (Mar 1958).
 29. S. H. Shenker and D. Stanford, *Journal of High Energy Physics* **2014**, p. 67 (Mar 2014).
 30. Y. Sekino and L. Susskind, *Journal of High Energy Physics* **2008**, p. 065 (2008).
 31. E. H. Lieb and D. W. Robinson, *Commun. Math. Phys.* **28**, p. 251 (1972).
 32. M. Cheneau, P. Barmettler, D. Poletti, M. Endres, P. Schauß, T. Fukuhara, C. Gross, I. Bloch, C. Kollath and S. Kuhr, *Nature* **481**, 484 EP (Jan 2012).
 33. B. Swingle, G. Bentsen, M. Schleier-Smith and P. Hayden, *Phys. Rev. A* **94**, p. 040302 (Oct 2016).
 34. D. A. Roberts and B. Swingle, *Phys. Rev. Lett.* **117**, p. 091602 (Aug 2016).
 35. M. Žnidarič, T. c. v. Prosen and P. Prelovšek, *Phys. Rev. B* **77**, p. 064426 (Feb 2008).
 36. R. Fan, P. Zhang, H. Shen and H. Zhai, *Science Bulletin* **62**, 707 (2017).
 37. J. Li, R. Fan, H. Wang, B. Ye, B. Zeng, H. Zhai, X. Peng and J. Du, *Phys. Rev. X* **7**, p. 031011 (Jul 2017).
 38. M. Gärttner, J. G. Bohnet, A. Safavi-Naini, M. L. Wall, J. J. Bollinger and A. M. Rey, *Nature Physics* **13**, 781 EP (May 2017), Article.
 39. E. Iyoda, K. Kaneko and T. Sagawa, *Phys. Rev. Lett.* **119**, p. 100601 (Sep 2017).
 40. M. Nakahara, Y. Kondo, K. Hata and S. Tanimura, *Phys. Rev. A* **70**, p. 052319 (Nov 2004).
 41. Y. Kondo and M. Bando, *Journal of the Physical Society of Japan* **80**, p. 054002 (2011).

24 *Y. Kondo & M. Matsuzaki*

42. T. Ichikawa, M. Bando, Y. Kondo and M. Nakahara, *Philosophical Transactions of the Royal Society of London A: Mathematical, Physical and Engineering Sciences* **370**, 4671 (2012).
43. Y. Kondo, M. Nakahara and S. Tanimura, Liquid-state nmr quantum computer: Hamiltonian formalism and experiments, in *Physical Realizations of Quantum Computing: Are the DiVincenzo Criteria Fulfilled in 2004?*, eds. M. Nakahara, S. Kane-mitsu, M. M. Salomaa and S. Takagi (World Scientific, Osaka, Japan, May 2006).
44. Y. Kondo, Liquid-state nmr quantum computer: Working principle and some examples, in *Molecular Realizations of Quantum Computing 2007*, eds. M. Nakahara, Y. Ota, R. Rahimi, Y. Kondo and M. Tada-Umezaki, Kinki University Series on Quantum Computing, Vol. 2 (World Scientific, 2009).
45. K. Kraus, *Annals of Physics* **64**, 311 (1971).
46. H. Barnum, M. A. Nielsen and B. Schumacher, *Phys. Rev. A* **57**, 4153 (Jun 1998).
47. E. Knill, R. Laflamme, R. Martinez and C. H. Tseng, *Nature* **404**, 368 EP (03 2000).